Conceptual design and evaluation of an optical sensor for wide-area high-voltage metering and protection applications

Grzegorz Fusiek and Pawel Niewczas
Department of Electronic and Electrical Engineering, University of Strathclyde, Glasgow, United Kingdom
g.fusiek@strath.ac.uk

Abstract— This paper considers the design of a fiber-optic voltage sensor for applications in the field of wide area monitoring, protection and control of high voltage power networks. The proposed 132-kV sensor, combining a capacitive voltage divider (CVD) and an optical medium voltage transducer (MVT), was theoretically evaluated through software simulations and its expected performance was assessed based on the operational requirements specified by the IEC standards for electronic voltage transformers. The simulation results suggest that the sensor, when fabricated, should be capable of meeting the requirements for metering and protection classes specified by the IEC 60044-7 standard.

Keywords— Fiber Bragg grating, optical voltage sensor, power system instrumentation, capacitive voltage divider, piezoelectric transducer

I. INTRODUCTION

Electricity distribution networks are essential to the wide-area power systems. The distribution grid combines overhead lines, underground cables, and step-down transformers to distribute the electrical power to the primary and secondary customers. In Europe, the distribution system voltage levels are between 0.4 kV and 225 kV, and in the UK distribution network, typical voltage levels are 0.4/11/33/132 kV [1].

Among many problems related to the electrical network functionality and stability are temporary or permanent faults. Temporary faults cause no damage to the electrical equipment and lead to temporary power outages. Permanent faults cause failure of the system equipment and lead to blackouts with durations sometimes reaching several hours. Temporary faults constitute the majority of faults in overhead distribution systems [2], [3]. Around half of the faults are caused by abnormal weather conditions such as lightning strikes. Lightning events usually cause temporary faults on distribution networks but some are causing permanent damage to the equipment [2]–[4]. Therefore, the equipment needs to be protected with surge arresters or be furnished with sufficient insulation that meets the relevant industry standards [2], [5].

Wide-area monitoring, protection and control systems (WAMPACS) play an important role in restraining the propagation of large disturbances and the prevention of blackouts in power networks [6], [7]. WAMPACS offer the increased network visibility, improved reaction time to the network demands, and improvements to the network reliability and security of energy generation, transmission and distribution [6], [7]. Novel sensor systems capable of providing remote and distributed voltage and current measurements while remaining cost-competitive with the current technology are desired for the developing WAMPACS technologies.

A range of photonic voltage and current sensors utilizing fibre Bragg grating (FBG) sensors and piezoelectric transducers was previously proposed by the authors to enable multiple, remote, distributed, passive current and voltage measurements over long distances that can be applicable to a wide range of metering and protection applications [8]–[12]. This included variants of the core technology from using low-voltage "soft" piezoelectric transducers to measure the output of a conventional CT or Rogowski coil for current measurement, through to using the same approach for sensing the secondary voltage of a capacitor divider to achieve voltage measurement at 132 kV [11] to direct voltage measurement at medium voltage by using larger "hard" piezoelectric (PZT) transducers that are capable of being exposed to multi-kV-level voltages [10], [12].

The key motivation of the work presented in this paper is to realize a high voltage photonic sensor that is based on a hard piezoelectric transducer. Hard piezoelectric materials can be operated at higher voltages and are known to demonstrate better linearity, smaller hysteresis, and better short- and long-term stability than the soft counterparts. Previous tests showed that the effects of the aging and de-aging (sensitivity changes) in the soft PZT are worse than those in the hard PZT [13], [14], which is especially important at rapid signal changes, like those during faults or lightning impulse events. However, the overvoltage protection of hard piezo components presents a greater challenge.

Consequently, in this paper, we concentrate on the design and theoretical evaluation of the high voltage optical voltage senor (HV OVS) combining a capacitive voltage divider and a hard piezoelectric transducer to achieve an improved sensor performance than was attained with its predecessor. We assess the transducer capability to withstanding the standard lightning impulse voltage and its potential to comply with metering and protection class requirements according to IEC 60044-7 [5].

Research presented in this paper was supported by the Innovate UK (project number 105638). All data underpinning this publication are openly available from the University of Strathclyde KnowledgeBase at https://doi.org/10.15129/5b35e95e-8650-43a8-a9f5-f8085c31d75c

II. Optical Voltage Sensor Design

A. Sensor voltage requirements

The proposed optical voltage sensor requires to be connected between one line of a 50-Hz 132-kV system and earth, and its rated voltage is equal to 76 kV with the rated voltage factor of 1.2 applicable to measurements between phase and earth on a continuous basis. Additionally, the device must withstand the rated power-frequency voltage of 275 kV and the rated lightning-impulse voltage of 650 kV [5].

B. Design criteria for photonic voltage transducer

When designing a voltage transducer, a decision about the use of either soft or hard piezo materials needs to be taken depending on the component operating voltage level. Soft PZT materials have higher piezoelectric charge coefficient (d_{33}) than hard PZT materials allowing to generate greater strain at the same length of the component, but they suffer in a greater degree from aging and de-aging effects than hard PZTs [13], [14]. The aging effect is characterized by spontaneous decay of the material properties with time while de-aging process allows for the reversal of the certain material degradation in existence of strong bipolar electric fields or heat above the Curie temperatures. Both lead to the changes in the sensor sensitivity. The phase displacement between input and output signals is greater in soft PZTs due to wider hysteresis and increased capacitance. The hard PZT materials are known to demonstrate better linearity than the soft PZTs. It is also expected that long-term performance of hard PZTs is more stable than the soft PZTs due to the more stable material properties of the hard PZT transducers [13], [15], [16]. However, the design of the HV PVT utilizing hard piezo components seems to be more challenging.

There are two contrary requirements when selecting the material dimensions along the d_{33} direction. To maximize strain generated in the material, shorter lengths of the component are preferred, but at the same time the length should be maximized to keep the electric field in the material below permissible levels. A combination of the cross-section area and the length of the component will influence its capacitance and the resultant phase displacement between input and output signals and the transducer bandwidth.

In addition to the electrical performance of PZTs, their mechanical performance needs to be considered carefully to ensure that the compressive and tensile stress limits for the materials are not exceeded [10], [12], [14]. Both excessive electric field and stress in the material may lead to its depolarization or permanent damage. Therefore, the transducers require overvoltage protection which can be realized by means of additional electronic or mechanical components.

The direct use of a hard-piezo stack for measuring high voltage, a scaled-up version of the previous MV PVT design [10], [12], does not seem to be feasible for the HV PVT construction due to the requirements for the maximum permissible electric field in the PZT components and the stack dimensions. Since the PZT stack cannot be readily protected against overvoltage conditions, it must be designed to withstand power frequency and the lightning impulse voltages. As a result, at the rated voltage, the sensor would operate at voltage levels being only a fraction of the sensor maximum working range, and the size of the stack would not be feasible.

Therefore, in this design, it is assumed that a capacitive voltage divider (CVD) capable of delivering 1 kV rated output will be used and the divider output will be monitored by a hard piezoelectric transducer. It should be noted that this level of voltage is perceived as manageable in terms of insulation and construction requirements.

C. Medium voltage transducer

To simplify the sensor construction, it is assumed that a single piezoelectric component will be used. Its length should be adequate to accommodate an FBG and ensure that the electric field and stress levels in the material are below the recommended limits. It is also assumed that electrical field is set up along the length of the piezoelectric component, in parallel with the FBG.

Since a standard FBG has a length of approximately 7-10 mm, the length of the piezo component should be at least 20 mm to allow for installation of additional FBG supporting arms [17].

It should be noted that, for example, strain generated in the material having 20 mm length will be larger than that in the 25 mm component for the same voltage applied across the electrodes. This is because electric field strength is inversely proportional to the gap between the electrodes (or piezoelectric transducer length). The diameter of the component will influence its capacitance which will increase for larger diameters. The mechanical performance of the piezo will also be affected due to the weight of the component. By choosing smaller piezo components working in longitudinal mode of operation, more even stress distribution in the material might be achieved.

The proposed construction of a medium voltage transducer is shown in Fig. 1.

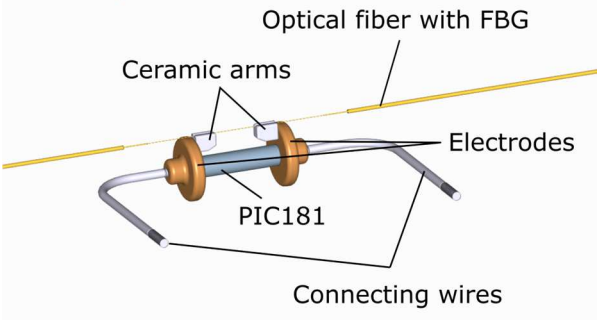

Fig. 1. Medium voltage transducer.

In the proposed design, the FBG sensor is suspended between two ceramic arms attached to two metallic electrodes sandwiching a cylindrical block of PIC181 material from Physik Instrumente (PI) [14]. The PIC181 component has a length of 20 mm and its diameter is 5 mm. It is proposed that the piezoelectric element and the ceramic arms are fixed to the electrodes using thin layers of a conducting epoxy while the fiber is attached to the arms using UV epoxy. Strain proportional to the input voltage is imparted to the FBG by the piezoelectric stack. The MVT construction ensures twofold

strain amplification [17]. To avoid the piezoelectric component depolarization and permanent damage its nominal voltage was chosen to be 1 kV as mentioned earlier. The compressive and tensile stress limits for the material are 100 MPa and 10 MPa, respectively while the permissible electric field limit is 2.5 kV/mm [10], [12], [14].

In the absence of mechanical or thermal stress in the piezoelectric material, the strain (i.e. relative elongation $\Delta L/L$) induced by an external electric field, E, is given by

$$\varepsilon = \frac{\Delta L}{L} = d_{33}E = d_{33}\frac{V}{L} \quad (1)$$

where L is the length of the rod, d_{33} is the longitudinal piezoelectric charge coefficient, and V is the voltage applied along the poling direction.

The series resonance frequency, f_s, for a piezoelectric disc with the voltage applied across its length can be calculated from the following equation:

$$f_s = \frac{N_{3s}}{L} \quad (2)$$

where N_{3s} is the series frequency constant and L is the length of the material, while the parallel resonance can be calculated as

$$f_p = \frac{N_{3p}}{L} \quad (3)$$

where N_{3p} is the parallel frequency constant. The above equations are good approximations for longitudinal operation of the component when $L >> OD$ (outside diameter) [14]. The fixing of the component, damping, and any losses are not considered here.

In positioning systems (standard application for piezoelectric transducers), at the frequencies working well below the resonance, the phase response of the actuator in degrees at frequency f can be approximated by [14]

$$\varphi \approx 2arctan\left(\frac{f}{f_0}\right) \quad (4)$$

The time required for the piezoelectric actuator to reach its nominal displacement at a sudden voltage change is approximately one third of the period of the resonant frequency:

$$T_{min} \approx \frac{1}{3f_0} \quad (5)$$

Based on the above theoretical equations, a rough estimation of the expected sensor parameters can be performed. Assuming a nominal voltage of 1 kV for the sensor, the electric field of 0.07 kV/mm can be expected in the PZT component, nearly two orders of magnitude lower than the permissible limit of 2.5 kV/mm [14]. Strain in the material at a nominal voltage of 1 kV is 18.7 με, resulting in the wavelength shift of 45 pm.

The theoretical values for the series and parallel resonant frequencies are 78.7 kHz and 99 kHz. Since the series resonant frequency is approximately 80 kHz, the component can reach its full displacement in approximately 4.2 μs after the driving voltage change, and the theoretical phase response is 0.07 degrees or 4 minutes at 50 Hz signals.

Based on the PIC181 dimensions and specifications, the component capacitance was calculated to be 10.4 pF and its resistance can be assumed 200 MΩ [10], [12], [14].

The transducer will be housed in a suitable package. Voltage input to the piezoelectric stack will be provided through two connecting wires as shown in Fig. 1, and metallic pins isolated from the package (not shown in the figure). The details of the package design are beyond the scope of this paper and will be focus of the future work.

The sensor can be interrogated remotely by measuring the peak wavelength reflected by the FBG, which shifts in proportion to the strain and hence applied voltage due to the change in period of the grating. By tracking the instantaneous peak wavelength, the voltage input can be reconstructed, and by tracking the average wavelength, local sensor temperature can be derived that can be used for temperature compensation of the sensor voltage readings.

The MVT has been designed with the requirements of environmental isolation, long-term reliability, and potential for mass production in mind.

D. Capacitive voltage divider

The proposed configuration for a high voltage (HV) capacitive voltage divider is shown in Fig. 2. The role of the capacitive voltage divider is to reduce the high voltage to the level that can normally be handled by the MVT. To bring the voltage down from ~76 kV to ~1 kV, the voltage division ratio of 76 was chosen. Assuming the MVT capacitance of 10.4 pF, the practical values of capacitors C_1 and C_2 were chosen as 1 nF and 75.2 nF, respectively.

It is expected that a bespoke CVD will be housed in a single HV composite insulator and will be provided by an external supplier. To offer access to the medium voltage output, the divider will be interfaced with the MVT placed in a suitable enclosure at ground level, and the access to the CVD medium voltage terminal will be provided inside the enclosure. The sensor will additionally be potted in a dielectric gel to reduce electric field strength around the sensor.

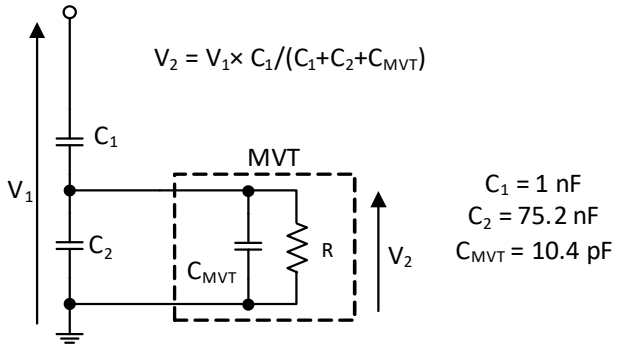

Fig. 2. HV divider diagrams: MVT measuring output voltage of a HV-to-MV divider. The dividing ratio is 76 assuming the MVT capacitance of 10.4 pF.

The CVD will have to comply with the requirements for the power frequency and lightning impulse withstand voltages and partial discharge limits set by the relevant IEC standards.

III. Software Simulations

For the analysis presented below, only the voltage delivered from the CVD output and apparent across the MVT terminals is considered. The stability of the CVD division ratio and other effects related to the CVD operation are not discussed here.

A. Model description

To verify the expected MVT performance at the nominal voltage and at the lightning impulse, finite element analysis (FEA) was performed in COMSOL Multiphysics® software.

During the simulations, one of the sensor electrodes was electrically grounded while the other was connected to a terminal voltage. The poling direction for the component was replicated from the real component and aligned with the *z* positive direction. This means that when the material was compressed in the *z* direction, the terminal voltage was negative (Fig. 3b). For negative voltages applied to the top electrode, the material will be tensioned as shown in Fig. 3d [12], [18].

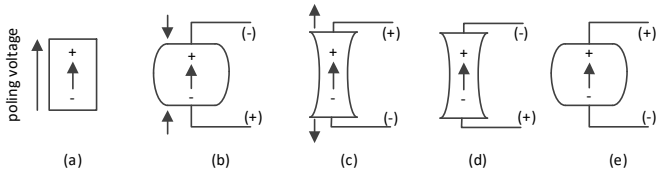

Fig. 3. Reaction of a piezoelectric component to applied force or voltage [12], [18]: poling direction (a), compression applied to the material in the poling direction generates voltage of the same polarity as the poling voltage (b); tension applied to the material in the poling direction generates voltage of the opposite polarity to the poling voltage (c); voltage of the same polarity as the poling voltage causes the material extension in the direction of the poling voltage (d); voltage of the opposite polarity as the poling voltage causes the material contraction in the direction of the poling voltage (e).

The component performance was analyzed for the resonant frequency, electric field distribution, and stress levels in the material. Representative examples of the simulation results are presented in the sections below.

B. Frequency domain response

To verify the FEA material model in the frequency domain study, a single PIC181 component impedance spectrum was simulated based on the material matrix data provided by the manufacturer. For this simulation, the component was not fixed at all and the gravity, damping or attachments were not included. The input voltage was a sinewave with an amplitude of 1 V. The frequency sweep was performed from 1 kHz to 160 kHz with 0.2 kHz steps. The absolute value of impedance was calculated from the complex admittance based on the terminal voltage and the piezoelectric material properties using global variables in COMSOL.

Based on the PIC181 properties specified by the manufacturer [14], the theoretical serial and parallel resonance frequencies for a rod with a length of 20 mm and a diameter of 5 mm modeled in COMSOL are 78.2 kHz and 98.5 kHz, respectively. Both resonance frequencies can clearly be seen in Fig. 4, where the component impedance spectrum received from the manufacturer is compared with the COMSOL simulation results. The experimental frequencies are slightly different than the theoretical ones at approximately 80 kHz and 96 kHz for serial and parallel resonances, respectively. The measurements were done with a Keysight 4294A with the component coaxially fixed with minimal force and with a voltage of 1 V (peak-to-peak) across the component. The observed differences in the resonant frequencies can be attributed to the tolerances for the material specifications and the measurement accuracy. Nevertheless, considering the FEA limitations and the tolerance on the material specifications, the results seem to be a reasonable approximation of the expected piezo element response.

The next simulation was performed for the PIC181 component fixed at one end while the other end could move in z direction only. The impedance spectrum is shown in Fig. 5.

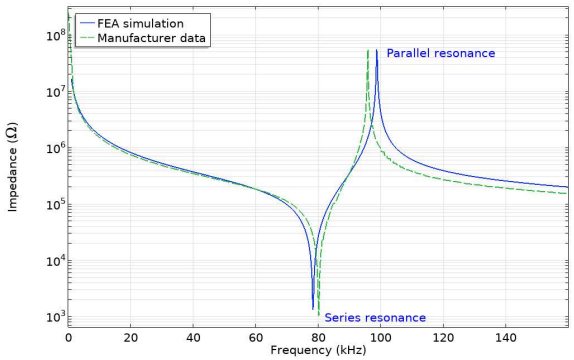

Fig. 4. Absolute value of impedance for an unfixed 20 mm long PIC181 element with 5 mm diameter simulated in COMSOL Multiphysics® compared to the impedance spectrum received from the manufacturer [14].

Evidently, the resonant frequencies were reduced from the first series resonance being at around 78 kHz in case of unfixed component to around 40 kHz when it is fixed. The results agree with the manufacturer statement that the resonant frequencies specified for longitudinal stack actuators listed in their datasheets apply to operation when the components are not clamped. For arrangements with unilateral clamping, the value must be divided in half [14].

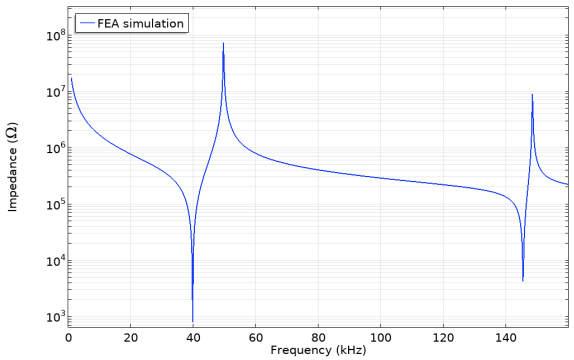

Fig. 5. Absolute value of impedance for a 20 mm long PIC181 element with 5 mm diameter simulated in COMSOL Multiphysics®. The element was fixed at one end.

Clearly, the way of fixing the component modifies the resonance frequencies, and hence, the piezo response time and phase. Therefore, this fact should be considered carefully during the design of the sensor arrangement in its packaging.

C. Lightning impulse requirements

IEC 60044-7 requires electronic voltage transformers (EVTs) to undergo 1.2/50 µs lightning impulse tests for devices with the highest voltage for equipment, U_m, of 3.6 kV and above [5]. The device under test (DUT) is expected to withstand 15 positive and 15 negative consecutive impulses.

As highlighted before, for the devices that are intended to be installed on 132 kV networks, the standard requires the devices to withstand lightning impulses with 650 kV peak voltage.

To model the expected electrical field distribution and stress levels in the PIC181 component during such events, a simulation of the circuit presented in Fig. 2 was performed in MATLAB. The relevant voltage waveforms with peaks at 650 kV (V_1) at the input of the CVD and at 8.5 kV (V_2) across the MVT are shown in Fig. 6.

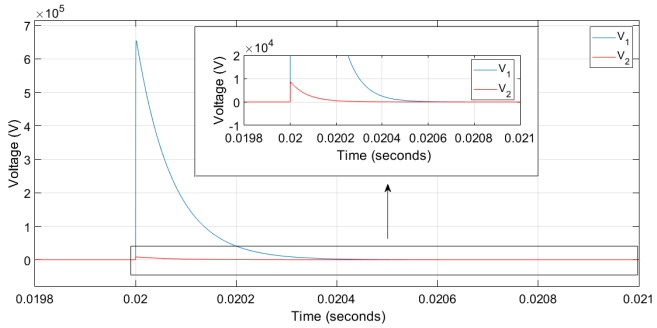

Fig. 6. Simulated CVD output voltage at the 650 kV lightning impulse.

The V_2 waveform was then transferred to COMSOL and used in the electrical field distribution and stress levels modeling as described below.

D. Electrical field modeling

For modeling the electric field distribution around the MVT, the sensor was set to be surrounded by a dielectric gel with a dielectric strength of 23 kV/mm and dielectric constant of 2.7.

The electrical field distribution around the sensor at a voltage of 8.5 kV is shown in Fig. 7.

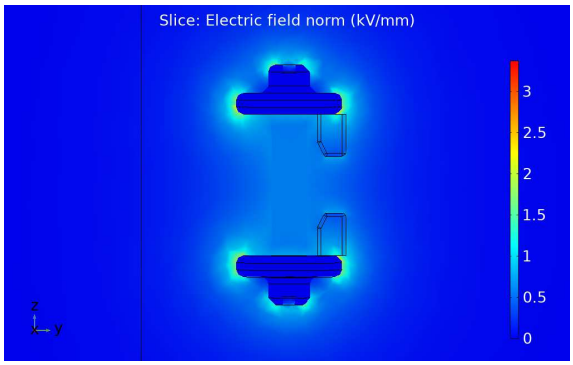

Fig. 7. Electric field distribution in the undamped piezoelectric component when subjected to 8.5 kV.

As can be seen, the higher fields are moved away from the piezo thanks to the electrodes with a diameter 3 times larger than the diameter of the PIC181 component. Also, designing the electrodes and the ceramic arms rounded with a 1 mm radius helped to minimize the electrical stress around the components with different dielectric constants and further improve the electric field distribution [17]. The field in the component is nearly 0.6 kV/mm which is well below the 2.5 kV/mm limit for the material. At a nominal voltage of 1 kV, the maximum field in the component is 0.07 kV/mm and the maximum electric field of 0.25 kV/mm can be expected at a power frequency withstand voltage of 5.1 kV.

It should be borne in mind that the performance of piezoelectric materials over time is influenced by operating temperature, voltage levels, and humidity. Therefore, the maximum electric field expected during the piezoelectric transducer operation should be selected with a sufficient margin in the transducer design process which is satisfied here.

E. Stress and strain modeling

As discussed earlier, due to the rapid change in voltage during a lightning impulse event, the piezoelectric component will undergo a shock that may result in large mechanical oscillations. Stress in the material can breach the recommended tensile stress limits for the material, potentially resulting in physical damage.

To assess the expected stress and strain levels in the material during the lightning impulse events, the relevant simulations were performed in COMSOL. Since it was assumed that the piezoelectric component will be attached to the electrodes with thin layers of a conducting epoxy as mentioned previously, it was also assumed that there will be no movement of the piezo element surface in the radial direction of the electrodes. The element could move in z direction freely and could be deformed in all directions in between the electrodes. The strain and stress levels were measured on the surface of the material in the center between the electrodes. The simulation results when a positive and negative impulses are applied to the material are shown in Fig. 8 and Fig. 9.

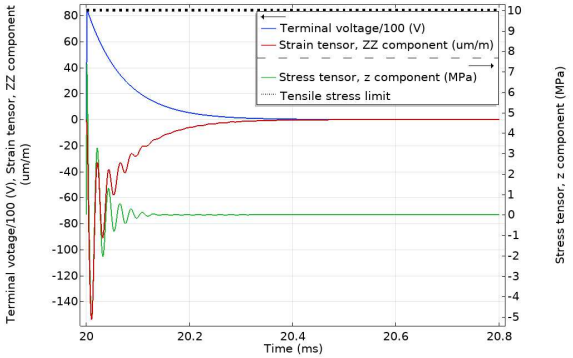

Fig. 8. Stress and strain in the undamped piezoelectric component when subjected to 8.5 kV positive lightning impulse. The tensile stress limit of 10 MPa is marked by a black dotted line.

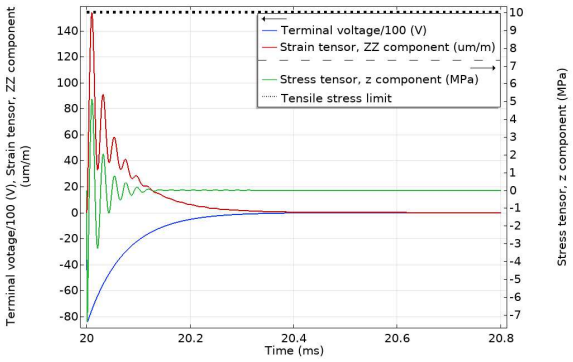

Fig. 9. Stress and strain in the undamped piezoelectric component when subjected to 8.5 kV negative lightning impulse. The tensile stress limit of 10 MPa is marked by a black dotted line.

As can be seen in the figures, the stress levels in the material are in both cases below the 10 MPa limit and the component should not be damaged during the lightning impulse event.

F. Measurement errors estimation

To assess the suitability of the sensor for protection and metering purposes, the measurement errors for 50 Hz voltage waveforms with amplitudes of 2%, 5% and between 80% and 120% of the device rated voltage would have to be considered.

Since the 3P class for protective devices need to comply with the accuracy requirements at 2 % of the nominal voltage, the wavelength shifts below 0.9 pm would have to be detectable with the amplitude errors below ±6 %. As the expected FBG peak wavelength shift at the nominal voltage is 45 pm (rms), the interrogation system resolution needs to be below 0.2 pm (rms). This is achievable with the interferometric interrogation method such as that previously proposed by the authors in [19].

IV. CONCLUSIONS

In this paper, the design of an optical voltage sensor for distributed voltage measurements on high-voltage distribution networks (132 kV) utilizing a hard piezoelectric transducer has been presented. The sensor performance was evaluated theoretically by modeling the expected sensor performance in FEA software. The simulation results suggest that the electric field in the material during the lightning impulse of 650 kV should be well below the permissible limit. Also, the stress in the material should remain within the limits recommended by the manufacturer so that the component should not be damaged.

The measurement errors estimation has shown that the sensor has the potential to meet the requirements of the IEC 0,2 class for metering devices and 3P class for protective devices.

Future work will focus on designing a suitable packaging for the MVT ensuring that the isolation requirements are met, which will be followed by the sensor construction and testing.

REFERENCES

[1] Chin Kim Gan *et al.*, "Evaluation of alternative distribution network design strategies," in *IET Conference Publications*, 2009, no. 550 CP, pp. 690–690, doi: 10.1049/cp.2009.0923.

[2] L. Wang, "The Fault Causes of Overhead Lines in Distribution Network," *MATEC Web Conf.*, vol. 61, no. 2016, p. 02017, Jun. 2016, doi: 10.1051/matecconf/20166102017.

[3] M. Lehtonen, "Fault rates of different types of medium voltage power lines in different environments," *PQ2010 7th Int. Conf. - 2010 Electr. Power Qual. Supply Reliab. Conf. Proc.*, pp. 197–202, 2010, doi: 10.1109/PQ.2010.5549998.

[4] H. Haes Alhelou, M. Hamedani-Golshan, T. Njenda, and P. Siano, "A Survey on Power System Blackout and Cascading Events: Research Motivations and Challenges," *Energies*, vol. 12, no. 4, p. 682, Feb. 2019, doi: 10.3390/en12040682.

[5] IEC, "IEC 60044, Instrument transformers – Part 7: Electronic voltage transformers," 1999.

[6] A. G. PHADKE, P. WALL, L. DING, and V. TERZIJA, "Improving the performance of power system protection using wide area monitoring systems," *J. Mod. Power Syst. Clean Energy*, vol. 4, no. 3, pp. 319–331, Jul. 2016, doi: 10.1007/s40565-016-0211-x.

[7] V. Terzija *et al.*, "Wide-Area Monitoring, Protection, and Control of Future Electric Power Networks," *Proc. IEEE*, vol. 99, no. 1, pp. 80–93, Jan. 2011, doi: 10.1109/JPROC.2010.2060450.

[8] P. Orr *et al.*, "Distributed Photonic Instrumentation for Power System Protection and Control," *IEEE Trans. Instrum. Meas.*, vol. 64, no. 1, pp. 19–26, Jan. 2015, doi: 10.1109/TIM.2014.2329740.

[9] J. Nelson *et al.*, "Development and testing of optically-interrogated current sensors," in *2016 IEEE International Workshop on Applied Measurements for Power Systems (AMPS)*, 2016, pp. 1–5, doi: 10.1109/AMPS.2016.7602871.

[10] G. Fusiek, J. Nelson, P. Niewczas, J. Havunen, E.-P. E.-P. Suomalainen, and J. Hallstrom, "Optical voltage sensor for MV networks," in *2017 IEEE SENSORS*, 2017, vol. 2017-Decem, pp. 1–3, doi: 10.1109/ICSENS.2017.8234104.

[11] G. Fusiek, P. Niewczas, N. Gordon, P. Orr, and P. Clarkson, "132 kV optical voltage sensor for wide area monitoring, protection and control applications," in *I2MTC 2020 - 2020 IEEE International Instrumentation and Measurement Technology Conference, Proceedings*, 2020.

[12] G. Fusiek and P. Niewczas, "Photonic Voltage Transducer with Lightning Impulse Protection for Distributed Monitoring of MV Networks," *Sensors*, vol. 20, no. 17, p. 4830, Aug. 2020, doi: 10.3390/s20174830.

[13] M. Promsawat, B. Marungsri, N. Promsawat, P. Janphuang, Z. Luo, and S. Pojprapai, "Effects of temperature on aging degradation of soft and hard lead zirconate titanate ceramics," *Ceram. Int.*, vol. 43, no. 13, pp. 9709–9714, Sep. 2017, doi: 10.1016/j.ceramint.2017.04.145.

[14] PI, "Physik Instrumente Ltd." [Online]. Available: http://www.piceramic.com/product-detail-page/p-882. [Accessed: 18-Nov-2020].

[15] O. Guillon, F. Thiebaud, and D. Perreux, "Tensile fracture of soft and hard PZT," *Int. J. Fract.*, 2002, doi: 10.1023/A:1022072500963.

[16] M. Peddigari *et al.*, "A Comparison Study of Fatigue Behavior of Hard and Soft Piezoelectric Single Crystal Macro-Fiber Composites for Vibration Energy Harvesting," *Sensors*, vol. 19, no. 9, p. 2196, May 2019, doi: 10.3390/s19092196.

[17] G. Fusiek, P. Niewczas, and M. D. Judd, "Towards the development of a downhole optical voltage sensor for monitoring electrical submersible pumps," *Sensors Actuators, A Phys.*, vol. 184, pp. 173–181, 2012, doi: 10.1016/j.sna.2012.06.020.

[18] P. Paufler, "Fundamentals of Piezoelectricity," *Zeitschrift für Krist.*, vol. 199, no. 1–2, pp. 158–158, Jan. 1992, doi: 10.1524/zkri.1992.199.1-2.158.

[19] M. Perry, P. Orr, P. Niewczas, and M. Johnston, "Nanoscale resolution interrogation scheme for simultaneous static and dynamic fiber bragg grating strain sensing," *J. Light. Technol.*, vol. 30, no. 20, pp. 3252–3258, 2012, doi: 10.1109/JLT.2012.2213891.